Experimental Investigations on Anchorage of Rebars in UHPC

Ekkehard Fehling, Paul Lorenz, Torsten Leutbecher
Institute of Structural Engineering, University of Kassel, Germany

Designing reinforced UHPC concrete structures requires information about the bond-behavior of non-prestressed rebars. Determining the influence of the main parameters in test series is necessary, especially in order to acquire the basic information needed to develop design-regulations. Because of the high compression strength, UHPC-structures are often filigree. Therefore the concrete cover and the failure mode are the main parameters in these investigations. If fibers are used, it is important to know how they influence the bond behavior or if they can replace a transverse reinforcement. Further important parameters are the bar diameter, rib geometry, pouring direction of concrete and load direction. In the building practice, the relevant influences of the aforementioned parameters are important. The main intention is to find out the necessary bond length and concrete cover of non-prestressed rebars in UHPC under these parameters.

Keywords: anchorage, bond, UHPC, UHPFRC, Rebars

1 Introduction

The material UHPC exhibits compression strengths near those of construction steel, which enables a reduction of cross sections and the use of fewer resources. In terms of reinforcement corrosion, the high packing density and the high resistance against ingress of fluids and gases allows markedly smaller concrete covers. At the same time, minimum concrete cover requirements must be observed in order to ensure a secure anchorage. For this purpose, the differences in bond behavior in comparison with NSC must be explored. Through the load transfer from the deformed bar along the ribs in the concrete, struts are formed, which are balanced by a tensile ring. A failure of the tensile ring results in the formation of splitting cracks, which negatively affect the multiaxial state of stress on the ribs. Due to the fact that the increase in tensile strength in comparison with that of NSC is disproportionately lower than the increase in compression strength, the focus must be placed on tensile failure. It is known that fibers have positive effects on the tensile failure characteristics.

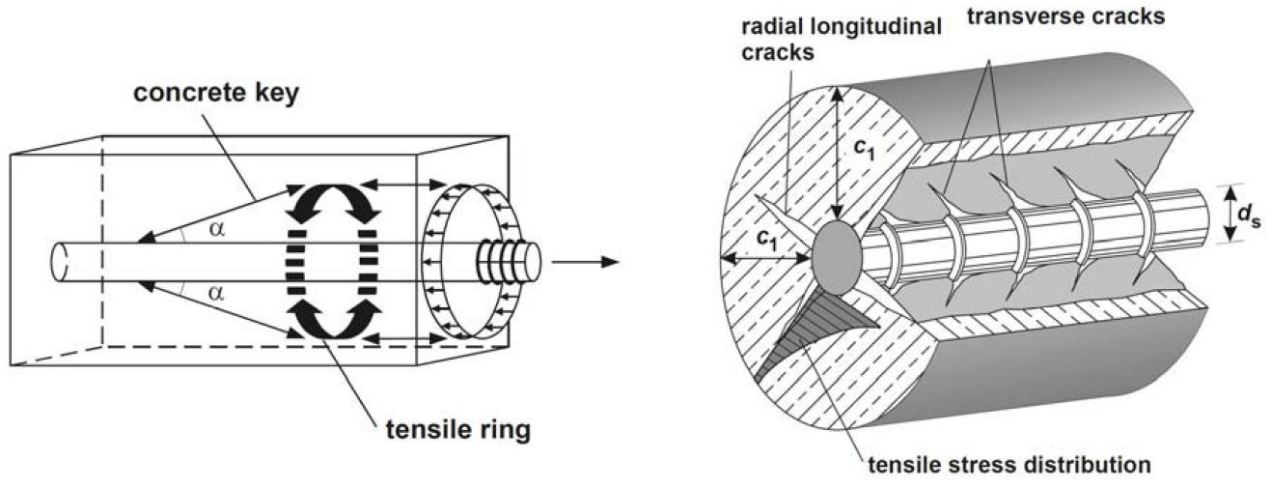

Figure 1: Spatial strut and tie model (left) and crack formation and concrete stresses (right) [7], [6].

Eligehausen et al. [8] examined various anchorage failure modes for NSC including pull-out, pry-out, splitting as well as combinations of these individual modes. Each mode was influenced by different parameters, for example confinement, the addition of fibers, relative rib area, concrete cover, casting direction etc. For this reason, the relevant parameters must be determined in order to assess anchorages for the ULS. These will be examined within the framework of a project funded by the German Research Foundation.

2 Current State of Research

From NSC to UHPC

Rehm [10] made one of the most fundamental contributions to questions concerning the bond between steel and concrete. In his work, he proposed to make initially all observations on a very short reinforcement element and established the differential relationship of bond.

Martin [12] provided, among others, approximations for the differential relationship of bond.

Fehling [1] developed a bond model, which worked with rheological, spring and friction elements [11] for both monotonic and cyclic loading.

Eligehausen et al. [8] examined anchorages in NSC. The obtained engineering models were introduced in the ETAG 001 [9]. Further studies for NSC are shown in [14].

Aarup et al. [4] examined the bond behavior of CRC (Compact Reinforced Concrete) on pull-out tests. Fiber contents of between 3 and 6 % by vol. were used. The concrete cover was 1.7 d_s (d_s = 8 mm) at a compression strength of 165 MN/m². A bond length of 6.3 d_s was sufficient to cause steel rupture prior to bond failure. In the case of smaller embedded lengths, pull-out failure with splitting cracks was observed. In addition he found that transverse reinforcement or lateral pressure is capable of causing a shortening of the bond length by 40 %. A lateral pressure of 5 % of the compression strength is sufficient to increase the bond strength by 60 %.

Based on fiber-reinforced fine-grained UHPC (DUCTAL®), Reineck and Greiner [5] determined a bond strength of between 43 and 51 MN/m² on ribbed bars with d_s = 4 mm and a concrete cover of 4.5 d_s. The bond length was 2 d_s. Pull-out tests were conducted on fiber-free fine-grained UHPC with a bond length of 3.3 d_s. This resulted in bond strengths of between 46 and 49 MN/m². Thereby no negative impact from failing fibers could be established. No splitting was observed.

Jungwirth [3] conducted pull-out tests on coarse-grained UHPC (CERACEM®) with threaded bars. The compression strength of the concrete was 190 MN/m² and the steel fiber content was 2 % by vol. (l_f/d_f = 20 mm/0.3 mm = 66.7). The slip was measured at the unloaded end. The result was an average bond strength of 59 MN/m² (see Fig. 1 and Tab. 1). He observed splitting failure at d_s = 20 mm with a concrete cover ratio of 3.5 d_s and showed that after splitting the load droped sharper in the post failure stage than without splitting.

Leutbecher [2] conducted tests to examine the bond behavior of reinforcement steel and high-strength steel in UHPC as well as in UHPFRC using the M1Q mixture [15]. Here, a total of 27 specimens were tested varying type of steel, the bar diameter, the concrete cover, and the casting direction. Additionally, a fiber content of 1 % by vol. was examined. It turned out that for high-strength steel and a concrete cover of 2.5 d_s the maximum bond stress, that means for high slip values, can be doubled by a addition of fibres i.e. a fiber content of 1 % by vol. in case of splitting crack formation. An increase of bond stress for values under 0.2 mm, however, is also achieved. Fiber addition showed no effect on the bond behavior if splitting crack formation could be excluded.

3 Own Tests on Anchorage of Rebars in UHPC

Experimental Program

The specimens consisted of a panel with constant length and width (see Fig. 2). The ribbed bar on which the bond behavior was to be observed was BSt 500 S with a diamameter of d_s = 12 mm. The embedded length l_b and the concrete cover c of this bar was modified. The casting direction was orthogonal to this bar and the concrete cover. The embedded length of the other bar (d_s =14 mm) was constant. In transverse direction to this bar, wire stirrups were used in order to avoid bond failure. To avoid a tensile failure between the two bars mentioned first, two additional bars with a diameter of d_s = 10 mm were arranged. The fine-grained UHPC M3Q with a fiber content of 1.5 % by vol. (l_f/d_f = 13 mm/0.19 mm = 68.4) and a compression strength of 170 MN/m² was used for all specimens. The formwork was stripped after 48 hours. Afterwards heat treatment at a temperature of 90 °C was applied to the specimens for 48 hours. An overview of the test program is presented in Tab 1. The investigated parameters were the bond length and the concrete cover.

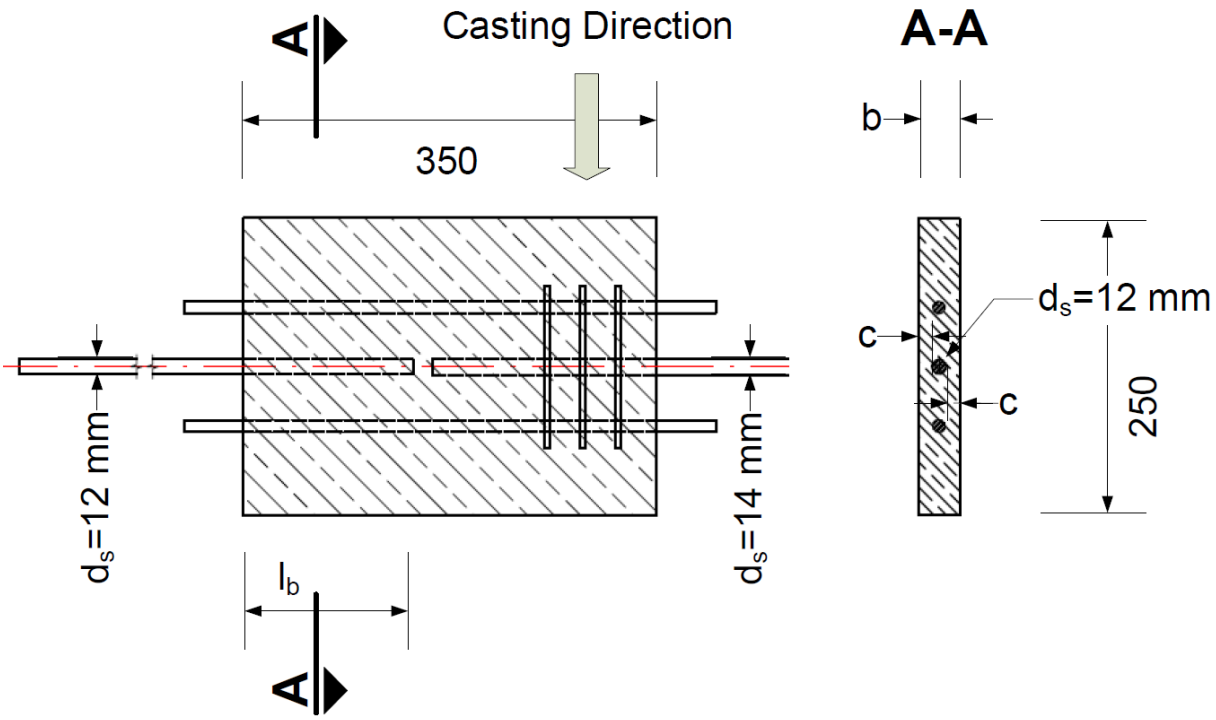

Figure 2: Specimen principle for ribbed bar Pull-Out with varying embedded lengths and concrete covers.

Table 1: Investigated parameters.

Name of the specimen		V12/1/4 V12/1/6 V12/1/8 V12/1/10 V12/1/12	V12/1.5/4 V12/1.5/5 V12/1.5/6 V12/1.5/8 V12/1.5/10	V12/2/2 V12/2/4 V12/2/5 V12/2/6 V12/2/8	V12/2.5/2 V12/2.5/3 V12/2.5/4 V12/2.5/5 V12/2.5/7
Concrete cover	c_{nom} / d_s	1	1.5	2	2.5
Bond length	l_b / d_s	4, 6, 8, 10, 12	4, 5, 6, 8, 10	2, 4, 5, 6, 8	2, 3, 4, 5, 7

Test Set-Up and Test Procedure

At first, the specimen was installed in the machine and the LVDT´s were applied. The ribbed bar on which the bond behavior was to be observed was free and not loaded at this time. After starting the measurement, this bar was pinched in the machine and the load-application was

started in a displacement-controlled way with a velocity of 0.1 mm/sec. The steel strain on this bar was obtained from the elongation Δl_b as measured by the LVDT-Group B with a measurement length l_b (see Fig. 3). The slip between the steel and the concrete was measured indirectly by the LVDT Group A. Here the measurement-length was l_a and the measured elongation was Δl_a. The slip was calculated from the measured values (see Eq. 3) using the assumption that the strains within l_a and l_b are identical. This assumption is valid for elastic behavior but not after onset of yielding.

$$\varepsilon_s = \Delta l_b / l_b \quad (1)$$

$$s + l_a \cdot \varepsilon_s = \Delta l_a \quad (2)$$

$$s = \Delta l_a - l_a \cdot \Delta l_b / l_b \quad (3)$$

Additionally, perpendicular to the direction of tensile force, splitting cracks were monitored on the concrete. Using three LVDT rows at the front side and three at the back of the specimen, information about the opening of the splitting crack could be obtained.

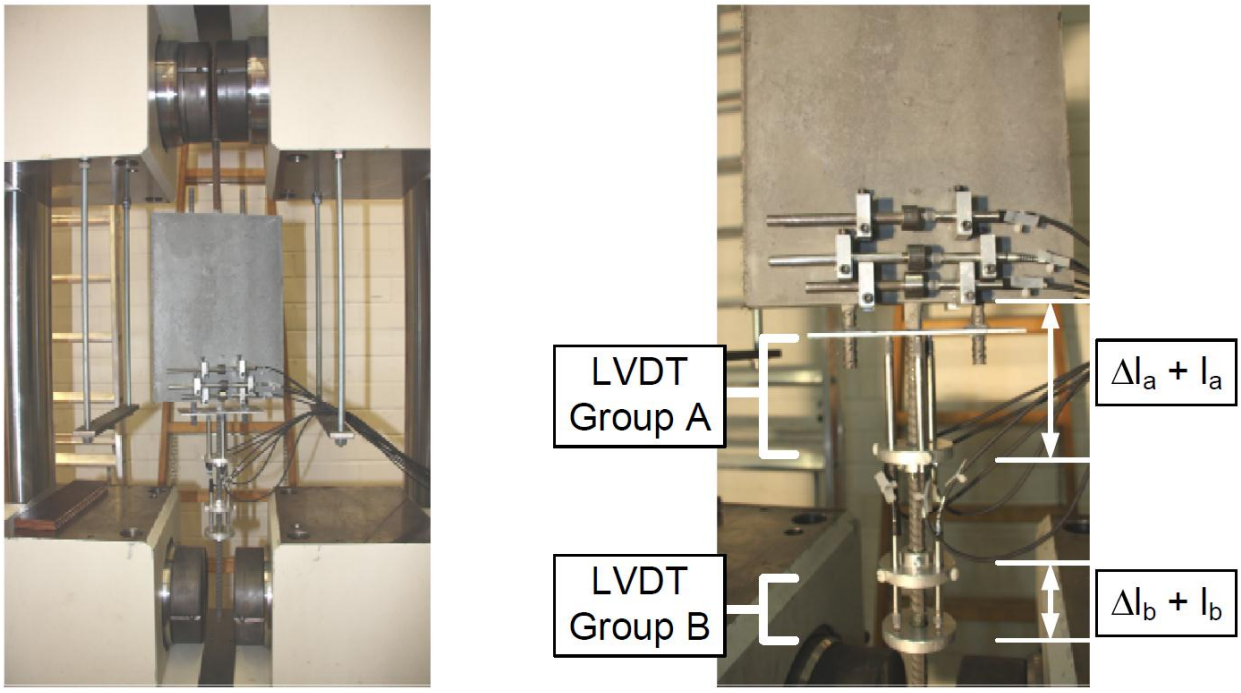

Figure 3: Specimen in testing machine (left), LVDT´s arrangement (right).

Results

During the test, various concrete failure modes could be observed and recorded. The major modes are illustrated in Fig. 4 and 5. In most cases, mixed failure modes developed. For this reason, failure modes were evaluated on the basis of the failure pattern and the remaining crack width. The results of the observations are depicted in Fig. 5. Here, especially the transition between concrete cone failure and V-type splitting can be seen to be very smooth. The overlap between V-type splitting and splitting means that V-type splitting occurred, in particular, near the load application, while splitting took place across the rest of the bond length. The yielding failure mode was observed when the reinforcement reached the yield plateau in the force-strain relationship.

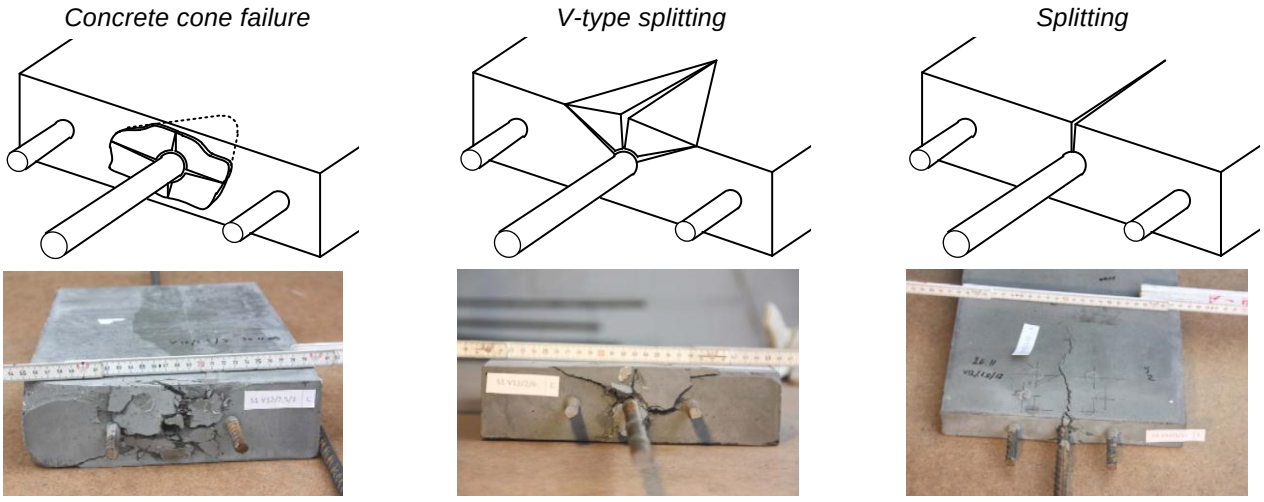

Figure 4: Concrete failure modes.

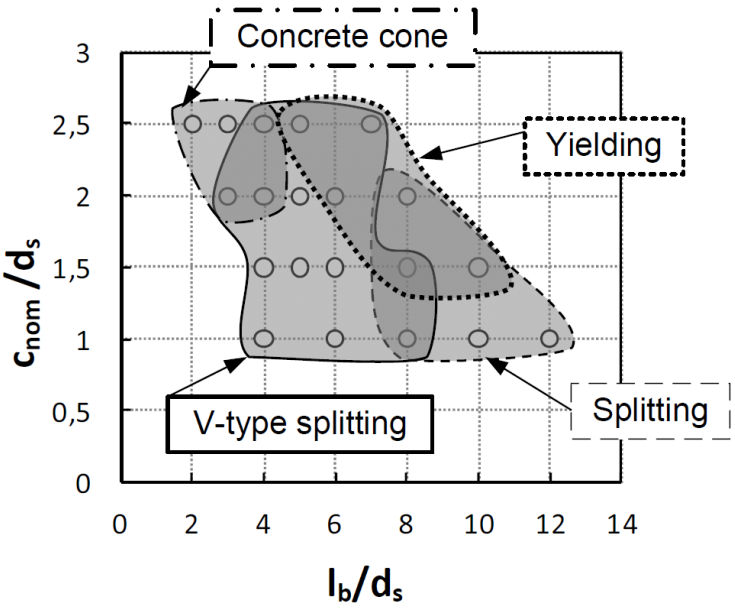

A transverse crack at the end of the bond-length was observed in all tests of this series

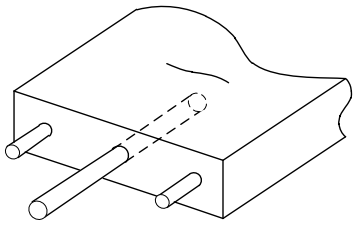

Figure 5: Major failure modes of the test specimens.

The steel stress-slip relationships of the individual tests are shown in Fig. 6 and Fig. 7. After reaching the yield plateau (two-point-dash line), the slip could be determined only qualitatively and should therefore be regarded with caution. The main parameters can be derived from the test denomination. „V12“ represents an anchorage of a bar diameter of 12 mm. The two-digit number without a decimal point after the letter “C” indicates the concrete cover ratio and the number after “L” the anchorage ratio.

With a concrete cover of c = 1 d_s and anchorage lengths of less than l_b = 8 d_s, increases in the maximum steel stress could be achieved by increasing the anchorage length (see Fig. 6). The failure mode observed here was V-type splitting. Increased anchorage lengths did not result in increasing failure load. The steel stress-slip relationships for the anchorage lengths 8 d_s, 10 d_s and 12 d_s are quite identical, even for slip values up to 14 mm (see Fig. 7). At the end of the test, the residual steel stress was between 50 and 100 N/mm². In the process of the test the steel stress remained below the yield plateau and the concrete failed due to splitting. This may be caused by a zipper-effect.

With a concrete cover ratio of 1.5 d_s, the steel stresses for $l_b \leq 6\ d_s$ remained below the yield stress. By increasing l_b until l_b = 6 d_s the maximum steel stresses increased (see Fig. 6). The

descending branch of the curves is almost identical for slip values between 4 mm and 15 mm (see Fig. 7). After reaching a slip value of 15 mm, a residual steel stress level of between 80 or 100 N/mm² could be observed and the test was aborted then. For $l_b = 8\ d_s$, a maximum steel stress (in the hardening stage) of 640 N/mm² was reached. Subsequently, the stress diminished with increasing slip. For $l_b = 10\ d_s$, the maximum steel stress was 670 N/mm². Here, the concrete failure switched from v-type splitting to splitting. For larger concrete covers, the concrete cone failure mode was observed more frequently. Nevertheless, predominantly mixed failure modes combining concrete cone and V-type splitting were observed (see Fig. 5).

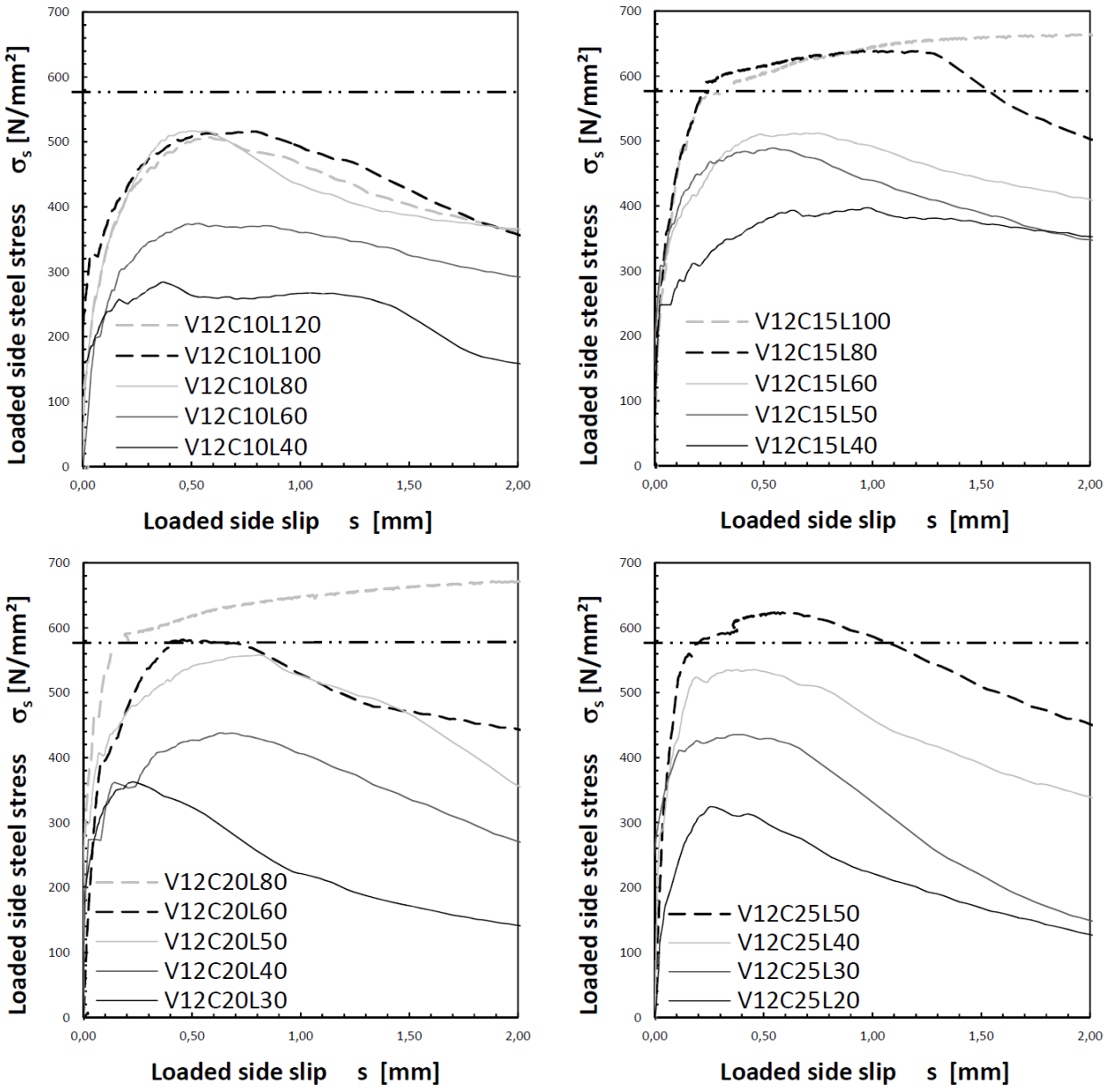

Figure 6: Steel stress-slip relationships for s ≤ 2,0 mm.

For $c = 2\ d_s$ and $l_b \leq 5\ d_s$, the steel stresses generally remained below the yield point. The yield point was exactly reached for $l_b = 6\ d_s$ whereas a steel stress in the hardening regime of 680 N/mm^2 was reached for $l_b = 8\ d_s$. The maximum steel stresses for $c = 2.5\ d_s$ and $l_b \leq 4\ d_s$ correspond approximately to those of $c = 2\ d_s$ and $l_b \leq 5\ d_s$. Here, the effect of the stiffer tensile ring from the larger concrete cover becomes obvious. This allows for an anchorage length of one diameter less and causes concrete cone failure.

For c = 2.5 d_s, $l_b \leq 3\ d_s$, pure concrete cone failure was observed. This type of failure resulted in a rapid decrease of the steel stress after reaching the peak load. At a slip value of 8 mm, the steel stress was almost zero.

For the concrete cover c = 2.5 d_s and the anchorage length $l_b = 5\ d_s$, it was possible to apply a steel stress of 620 N/mm². Due to a malfunction of the instrumentation, no slip values could be measured for the anchorage length $l_b = 7\ d_s$. However, a steel stress of 620 N/mm² was reached also for this specimen and the V-type splitting failure mode with yielding was observed (see Fig. 5).

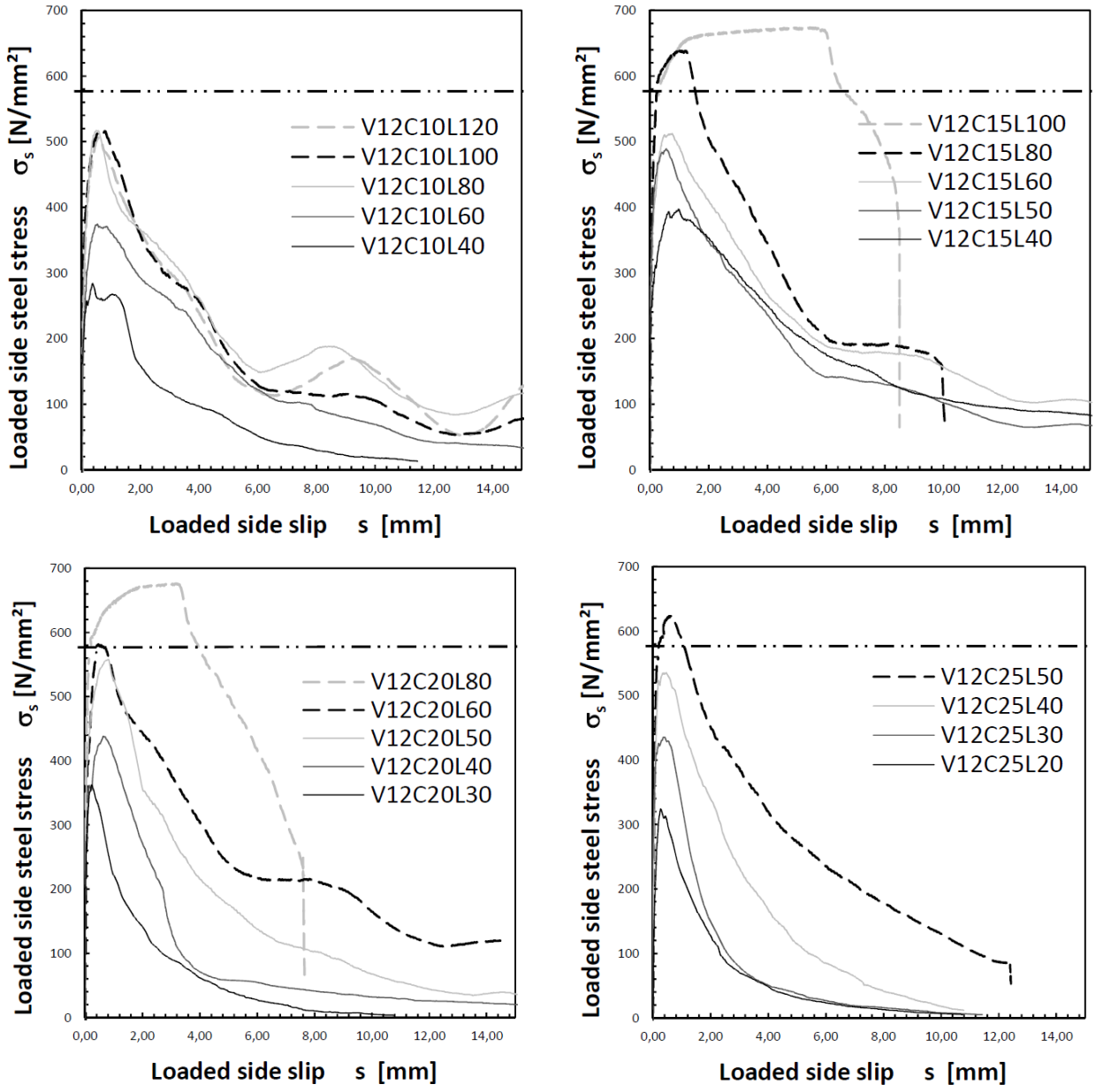

Figure 7: Steel stress-slip relationships for s ≤ 15,0 mm.

4 Conclusions and Outlook

In the case of concrete cone failure, the post failure behavior is rather brittle. Based on the assumption that the slip arises only from the opening of the cone shaped crack, it becomes evident that no or only very small forces can be transferred at a slip of $l_f /2 \approx 7$ mm. This is the reason why the steel stress diminishes so rapidly in this case. This type of failure, which is frequently seen with dowel connections, should be avoided. In the case of splitting and V-type

splitting, a more ductile post failure behavior can be obtained, which results from the crack direction and the formation of multiple cracks. Due to the activation of the fibers in the splitting crack, a certain confinement effect is preserved. Therefore, this post failure behavior is significantly influenced by the stress-crack opening behavior of the fiber-reinforced concrete.

Further questions require more detailed examination:

- How are the obtained relations between geometrical parameters and failure modes influenced by the diameter and the relative rib area of the rebar?
- How much transverse reinforcement is required in order to achieve a shortening of bond length at constant fiber contents?
- To what extent do fibers and transverse reinforcement ratio compliment each other?

To answer these questions further investigations should be made by varying the transverse reinforcement ratio, the diameter and the relative rib area of the bar.

References

[1] Fehling, E.: Zur Energiedissipation und Steifigkeit von Stahlbetonbauteilen unter besonderer Berücksichtigung von Rißbildung und verschieblichem Verbund. Dissertation, Darmstadt, 1990.

[2] Leutbecher, T.: Rissbildung und Zugtragverhalten von mit Stabstahl und Fasern bewehrtem Ultrahochfesten Beton (UHPC). Dissertation, Schriftenreihe Baustoffe und Massivbau, Heft 9, kassel university press GmbH, Kassel, 2008.

[3] Jungwirth, J.: Zum Tragverhalten von zugbeanspruchten Bauteilen aus ultra-hochleistungs-Faserbeton. Thèse N° 3429, Faculté Environment Naturel, Architectural et Construit, Ècole Polytechnique Fédérale de Lausanne, 2006.

[4] Aarup, B.; Karlsen, J.; Lindström, G.: Fiber reinforced high performance concrete for in-situ cast joints. Proceedings of International Symposium on High Performance Concrete, Orlando, Florida, USA, September 2000.

[5] Reineck, K.-H., Greiner, S.: Tests on ultra-high performance fibre reinforced concrete designing hot-water tanks and UHPFRC-shells. Ultra High Performance Concrete (UHPC), Proceedings of the Inernational Symposium on Ultra-High Performance Concrete, Schriftenreihe Baustoffe und Massivbau, Heft 3, kassel university press GmbH, Kassel, 2004.

[6] Holschemacher, K.; Weiße, D.; Klotz, S.: Bond of Reinforcement in Ultra High Strength Concrete. Proceedings of the International Symposium on Ultra High Performance Concrete, Kassel, 2004.

[7] Tepfers, R.: A Theory of bond applied to overlapped tensile reinforcement splices of deformed bars. Report 73-2, Chalmers University of Technology, Göteborg, 1973.

[8] Eligehausen, R.; Mallée R.; Silva, J.F.: Anchorage in Concrete Construction. Ernst&Sohn, Berlin, 2006.

[9] EOTA: ETAG 001. Guideline for european technical approval of metal anchors for use in concrete. 2007 -2011.

[10] Rehm, G.: Über die Grundlagen des Verbundes zwischen Stahl und Beton. DAfStb, Heft 138, 1961.

[11] Tue, N.: zur Spanungsumlagerung im Spannbeton bei der Rißbildung unter statischer und wiederholter Belastung. DAfStb, Heft 435, 1993.

[12] Martin, H.: Zusammenhang zwischen Oberflächenbeschaffenheit, Verbund und Sprengwirkung von Bewehrungsstählen unter Kurzzeitbelastung. DAfStb, Heft 228, 1973.

[13] fib Bulletin 55: Model Code 2010. First complete draft-Volume 1.

[14] Kurz, W.: Ein mechanisches Modell zur Beschreibung des Verbundes zwischen Stahl und Beton. Dissertation, Darmstadt, 1997.

[15] DFG SPP 1182: DFG Schwerpunktprogramm, Nachhaltiges Bauen mit ultra-hochfestem Beton.